Spontaneous chondroma formation in CD2-Cre-driven Erk-deficient mice

塩川, 萌

Short Communications

Spontaneous chondroma formation in CD2-Cre-driven Erk-deficient Mice

Running title: T-cell signature genes expressed in chondrocytes

Moe Shiokawa[1,2#], Xiuyuan Lu[1,2,3#], Yasunobu Miyake[4], Eri Ishikawa[1,2,3], Gilles Pagès[5], Jacques Pouysségur[5,6], Masato Ogata[7] and Sho Yamasaki[1,2,3,8]

[1]Division of Molecular Immunology, Medical Institute of Bioregulation, Kyushu University, Fukuoka, Japan
[2]Department of Molecular Immunology, Research Institute for Microbial Diseases, Osaka University, Suita, Japan
[3]Laboratory of Molecular Immunology, Immunology Frontier Research Center, Osaka University, Suita, Japan
[4]Division of Molecular and Cellular Immunoscience, Department of Biomolecular Sciences, Faculty of Medicine, Saga University, Saga, Japan
[5]Institute for Research on Cancer & Aging, Nice (IRCAN), CNRS, INSERM, Centre A. Lacassagne, University of Nice-Sophia Antipolis, Nice, France
[6]Medical Biology Department, Centre Scientifique de Monaco (CSM), Monaco
[7]Department of Biochemistry and Proteomics, Graduate School of Medicine, Mie University, Tsu, Japan
[8]Division of Molecular Immunology, Medical Mycology Research Center, Chiba University, Chiba, Japan

[#]Contributed equally to this study

Correspondence to: Sho Yamasaki
Department of Molecular Immunology, Research Institute for Microbial Diseases, Osaka University, Yamadaoka 3-1, Suita, Osaka 565-0871, Japan
Phone: +81-6-6879-8306, FAX: +81-6-6879-8308
E-mail: yamasaki@biken.osaka-u.ac.jp

Abstract

Lineage-specific Cre Tg mice are widely used to delineate the functions of genes in a tissue-specific manner. Several T cell-specific promoter cassettes have been developed, however, the activities of those promoters in non-T cells have not been investigated extensively. Here, we report that CD2-Cre-mediated deletion of Erk proteins by generating CD2-Cre × $Erk1^{-/-}Erk2^{flox/flox}$ ($Erk^{\Delta CD2\text{-}Cre}$) mice results in abnormal cartilage hyperplasia. Histological analysis revealed that this abnormality is caused by aberrant hyperplasia of chondrocytes. The presence of Erk-deficient T cells is not required for this chondroma formation, as it was similarly observed in the absence of T cells in CD3ε-deficient background. In addition, adoptive transfer of bone marrow cells from $Erk^{\Delta CD2\text{-}Cre}$ mice to WT recipients did not cause chondroma formation, suggesting that Erk-deficient non-immune cells are responsible for this abnormality. By tracing Cre-expressed tissues using a ROSA26-STOP-RFP allele, we found that the chondroma emitted RFP fluorescence, indicating that functional Cre is expressed in hyperplastic chondrocytes in $Erk^{\Delta CD2\text{-}Cre}$ mice. Furthermore, RFP^{+} chondrocytes were also found in Erk-sufficient background, albeit without aberrant growth. These results suggest that unexpected expression of CD2-driven Cre in chondrocytes generates Erk-deficient chondrocytes, resulting in hyperplastic cartilage formation. Recently, two independent reports showed that CD4-Cre-mediated Ras-Erk signaling ablation led to similar abnormal cartilage formation (Guittard, et al, *Front. Immunol.,* 2017; Wehenkel, et al, *Front. Immunol.,* 2017). Together with these reports, our study suggests that an unexpected link exists between T-like cell and chondrocyte lineages during ontogeny.

Introduction

A widely used tool for delineating the uncharacterized functions of genes in T cells is the mice in which Cre-expressing transgenes are placed under the control of promoters deemed to be T cell-specific, i.e. CD2, CD4 and Lck (1,2,3). To establish a mature T cell-specific transgenic mouse model, we previously generated a CD2-Cre transgenic line that expresses Cre specifically in mature T cells, but not in immature T cells or B cells (4,5).

The extracellular signal-regulated kinase (Erk) 1 and 2, also known as mitogen-activated protein kinase (MAPK) 3 and 1 respectively, are crucial components of Ras-MAPK pathways. Erk1 and Erk2 are expressed ubiquitously in mammalian cells, and are activated through a series of kinases by various stimuli including growth factors, cytokines and antigens. By phosphorylating their targets, Erk1 and Erk2 redundantly control proliferation and differentiation in many cell types (6,7). In chondrogenesis, however, Erk pathways play a negative regulatory role, as chondrocyte progenitor- or chondrocyte-specific Erk-deficient mice exhibit hyperplasia of chondrocytes and abnormal cartilage development (8,9,10). Conversely, forced activation of Erk by the introduction of active mutant MEK1 in chondrocytes led to an achondroplasia-like dwarf phenotype in mice (11).

In this paper, we report a spontaneous chondroma formation caused by the conditional deletion of Erk driven by CD2-Cre. Fate-mapping using fluorescent reporter RFP as well as histological analyses suggests that CD2 is unexpectedly expressed in some particular population of chondrocyte lineage and generates Erk-deficient

chondrocytes, which intrinsically contribute to chondroma formation.

Methods

Mice. Mature T cell-specific CD2-Cre (maT-Cre) Tg mice (4,5), Erk1$^{-/-}$ mice (12) and Erk2$^{flox/flox}$ mice (13) were generated previously. ROSA-tdRFP (ROSA26-STOP-RFP) reporter mice were provided by H-J. Fehling (14). CD3ε$^{\Delta5/\Delta5}$ mice were provided by B. Malissen (15). All mice were maintained in a filtered-air, laminar-flow enclosure and given standard laboratory food and water *ad libitum*. All animal protocols were approved by the Committee of Ethics on Animal Experiment, Faculty of Medical Sciences, Kyushu University and Animal Care and Use Committee of the Research Institute for Microbial Diseases, Osaka University, and performed in accordance with guidelines of Kyushu University and Osaka University.

Evaluation of symptoms. A 0-2 scoring system was used to evaluate the severity of hyperplasia (0, no symptom; 1, visible swelling; 2, obvious hard nodule). For the score of an individual mouse, the symptoms of all four feet were assessed separately, then the sum of the four values was used to indicate the score of the individual mouse. The scores of mice evaluated at the same age were averaged, and are shown in Figure 2A. For the incidence of the disease, mice that had at least one foot displaying symptom were counted.

Histology. For Hematoxylin and eosin (HE) staining, forefeet from WT and Erk$^{\Delta CD2\text{-}Cre}$ mice were fixed with 10% Formalin Solution (Wako, Osaka, Japan), washed with PBS, and decalcified with a solution of 10% sodium citrate and 22.5% formic acid. The

tissues were processed routinely, embedded in paraffin, sectioned and stained with hematoxylin and eosin. Sections were observed with a fluorescence microscope (BZ-9000, Keyence, Osaka, Japan).

For vertical observation of ear auricular cartilage, both sides of skin and connective tissues were removed from cartilage layer by forceps. The layer was washed with PBS, placed on glass slides and covered by coverslips. For the observation of cross sections, auricle was frozen with OCT compound (Sakura Finetek Japan), and sectioned by Cryostat (Leica Biosystems). RFP and bright-field images were acquired using the fluorescence microscope.

Imaging analysis. X-ray images were obtained using a microfocus X-ray imaging system (μFX-1000, FUJIFILM, Tokyo, Japan). Mice were sacrificed, fixed on an imaging plate, and exposed to 40 kV for 5 seconds (whole body) or to 20 kV for 5 seconds (hind feet). For detection of RFP fluorescence in nodules, the skin of the hind limbs from $Erk^{\Delta CD2\text{-}Cre}$ and $Erk^{\Delta CD2\text{-}Cre}$ × ROSA26-STOP-RFP mice was removed, and RFP signals were captured using a fluorescence stereomicroscope (M205FA, Leica MICROSYSTEMS, Wetzlar, Germany) with an excitation filter (BP 546 ± 10 nm) and an emission filter (BP 605 ± 70 nm).

RT-PCR analysis. For the isolation of chondrocytes, skin and connective tissues were removed from ear auricles and nodules with forceps. Total RNA was extracted from the tissues and the reverse transcripts were amplified with the following primers:

Sox9-forward, 5’-CAAGAAAGACCACCCCGATTACA-3’; Sox9-reverse, 5’-ACCC TGAGATTGCCCAGAGTGCT-3’; Col2-forward, 5’-GGAAGAGCGGAGACTACTG GATTG-3’; Col2-reverse, 5’-CATCGCCATAGCTGAAGTGGAAGC-3’; Acan-forwa rd, 5’-GGAGTTCGTCAACAAAAATGCTCAA-3’; Acan-reverse, 5’-CTCATGCCA GATCATCACCACACAG-3’; Col10-forward, 5’-TTCTGCTGCTAATGTTCTTGAC C-3’; Col10-reverse, 5’-GCCTTGTTCTCCTCTTACTGG-3’; CD2-forward, 5’-AGT GGATCATGGGCTTTGAG-3’; CD2-reverse, 5’-TGATGAGAAACGACAGTGGC-3’; CD4-forward, 5’-CACTGCATCAGGAAGTGAACC-3’; CD4-reverse, 5’-GGGG CCACCACTTGAACTAC-3’; CD3-forward, 5’-CACTGGTTCCTGAGATGGAGA-3’; CD3-reverse, 5’-GATGCGGTGGAACACTTTCT-3’; CD8-forward, 5’-GTTGGG GCAGTTGTAGGAAG-3’; CD8-reverse, 5’-TGTGAAGCCAGAGGACAGTG-3’; L ck-forward, 5’-CCGAGGGAGTCTTGAGAAAA-3’; Lck-reverse, 5’-CTTTATGCA GTGGTCACCCA-3’; GAPDH-forward, 5’-GCCGGTGCTGAGTATGTCGT-3’; GA PDH-reverse, 5’-AGATGATGACCCGTTTGGCT-3’.

Detection of TCRβ gene rearrangement. Genomic DNA was taken from the same nodule and ear chondrocytes that were used for RT-PCR analysis. The amplification was performed with the following primers:

Dβ1-forward, 5’-GCTTATCTGGTGGTTTCTTCCAGC-3’; Jβ1-reverse, 5’-GCAGA GTTCCATTTCAGAACCTAGC-3’.

Results and Discussion

Abnormal cartilage formation in CD2-Cre-mediated Erk-deficient mice

We previously established mature T cell-specific Cre (maT-Cre) Tg mice using the human CD2 promoter (4,5). In the current study, we crossed these Tg mice with Erk1-deficient ($Erk1^{-/-}$) and Erk2-floxed ($Erk2^{flox/flox}$) mice to create $Erk^{\Delta CD2\text{-}Cre}$ mice. During the breeding of these mice, we noticed that some nodules formed at the joints of the fore and hind feet of $Erk^{\Delta CD2\text{-}Cre}$ mice (Fig. 1A). Each nodule appeared to consist of hard components upon assessment by forceps palpation. Furthermore, X-ray spectroscopy reveals high-contrast material at the nodules, suggesting they contained cartilage and/or bone (Fig. 1B).

We next analyzed the histology of sections of the joint nodules using HE staining. In contrast to the normal organization of chondrocytes observed in WT mice, the cross section of nodules from $Erk^{\Delta CD2\text{-}Cre}$ mice revealed aberrant hyperplastic chondrocytes which appeared to be chondroma (Fig. 1C). This was also supported by the chondrocyte-characteristic gene expression, such as Sox9, Col2 and Acan. In particular, Col10, a hypertrophic chondrocyte marker was clearly detected in nodule (Fig. 1D). Of note, we did not observe an infiltration of inflammatory cells in the chondroma. These results suggest that the abnormal nodule formation in $Erk^{\Delta CD2\text{-}Cre}$ mice may result from the hyperplastic proliferation of chondrocytes that leads to anomalous cartilage growth without inflammation.

Erk-deficient T cells are not required for aberrant cartilage formation

We followed the severity of abnormal joints in $Erk^{\Delta CD2\text{-}Cre}$ mice as assessed by the disease score and noticed that the average score increased with age (Fig. 2A). To dissect the mechanism of the phenomenon, we examined its occurrence in WT, Erk1-deficient ($Erk1^{-/-}$), Erk2-deficient ($Erk2^{flox/flox}$ × CD2-Cre) and $Erk^{\Delta CD2\text{-}Cre}$ mice ($Erk1^{-/-}Erk2^{flox/flox}$ × CD2-Cre). More than 85% of $Erk^{\Delta CD2\text{-}Cre}$ mice older than 20 weeks developed chondromas, while WT, Erk1-deficient and Erk2-deficient mice showed no symptom (Fig. 2B). These results indicate that chondroma formation is specific to mice that lack Erk proteins in CD2-Cre-expressing cells.

We next asked whether Erk deletion in T cells is responsible for this phenomenon. To this end, we transferred bone marrow (BM) cells from $Erk^{\Delta CD2\text{-}Cre}$ mice into lethally irradiated WT mice to reconstitute Erk-deficient hematopoietic cells in an Erk-sufficient non-hematopoietic environment. Although Erk-deficient peripheral T cells were almost fully reconstituted in WT recipients (data not shown), none of the 15 recipient mice showed abnormal cartilage formation, even by 7 months after BM transfer (Fig. 2C). We further crossed T cell deficient $CD3\varepsilon^{\Delta 5/\Delta 5}$ mice with $Erk^{\Delta CD2\text{-}Cre}$ mice to directly clarify the role of Erk-deficient T cells in this abnormal cartilage formation. Surprisingly, abnormal cartilage formation similarly occurred even in the absence of T cells (Fig. 2D). Collectively, these results suggest that Erk-deficient T cells are not required for this abnormality; rather, Erk deletion in non-hematopoietic cells appears to be responsible.

Erk-deficient chondrocytes cause hyperplastic cartilage

To further address the question of what cells are responsible for the abnormality, we took advantage of fate-mapping analysis. The introduction of the ROSA26-STOP-RFP allele (14) into $Erk^{\Delta CD2\text{-}Cre}$ mice enables the tracing of cells expressing, or having expressed, Cre at the abnormal joints. Strikingly, upon analysis of the chondroma by fluorescence stereomicroscopy, we observed that most of hyperplastic cartilage area emitted bright red fluorescence (Fig. 3A).

To determine whether the RFP-positive tissue represented cartilage or bone, we removed the skin from the nodule and performed bright-field and fluorescence microscopy. The RFP-positive area was overlapped with the cartilage visualized as translucent area in bright-field, whereas 'white' bone tissues were RFP-negative (Fig. 3B). These results suggest that chondrocytes, but not osteocytes, expressed functional Cre recombinase, which led to the deletion of Erk and the expression of RFP in these cells. It has been previously reported that deletion of Erk in chondrocytes leads to their hyperproliferation (10,16). In line with this scenario, we speculate that the unexpected deletion of Erk in chondrocytes by CD2-driven Cre caused chondroma formation.

To investigate whether endogenous CD2 is expressed in chondrocytes, we examined the mRNA level of CD2 in the chondromas of $Erk^{\Delta CD2\text{-}Cre}$ mice. Remarkably, chondroma was found to be expressing considerable amount of CD2 mRNA, suggesting that not only CD2-driven transgene but also endogenous CD2 can be expressed in the chondroma (Fig. 3C). To exclude the possibility that the expression were due to the contamination of peripheral T cells, we evaluated the rearrangement of TCRβ genomic locus. In sharp contrast to splenic T cells having rearranged TCRβ genes, chondroma

had only non-rearranged germline band, thus suggesting that CD2 was expressed in chondrocytes (Fig. 3D).

We therefore examined the trace of CD2 expression and morphology of chondrocytes in other tissues from $Erk^{\Delta CD2\text{-}Cre}$ × R26-RFP mice. Fluorescence microscopic analysis clearly detected 'fate-mapped' RFP^+ chondrocyte clusters in the ear auricular cartilage, indicating that the expression of CD2 is not restricted to joint chondrocytes (Fig. 3E). Notably, these clusters were overlapped with the irregularly growing chondrocyte clusters in bright-field, suggesting that CD2-driven Erk deletion causes aberrant growth of chondrocytes in different locations. Intriguingly, in the auricular cartilage of Erk-sufficient R26-RFP mice, RFP^+ chondrocyte clusters were also clearly detected, albeit exhibiting normal morphology, inlayed among the RFP^- chondrocytes, suggesting that CD2 has been expressed in some specific chondrocyte population regardless of Erk expression (Fig. 3E).

These observations were also confirmed by cross sections of auricles. Again, RFP^+ chondrocytes appeared co-localized with hyperplastic chondrocyte clusters, which resulted in aberrantly shaped layer of auricular cartilage in Erk-deficient mice (Fig. 3F). By comparison, we could not observe any atypically arranged chondrocytes in the cross sections from Erk-sufficient mice (Fig. 3F), although some RFP^+ chondrocytes were detected as in Figure 3E.

As expected, we could detect substantial level of CD2 mRNA in the auricular cartilage in $Erk^{\Delta CD2\text{-}Cre}$ mice (Fig. 3G). However, it was only slightly detected in WT mice (Fig. 3G), suggesting that CD2 expression is not sustained during the development

of chondrocytes in the presence of Erk.

Taken together, these results suggest that 1) CD2 can be expressed in early stage of some specific chondrocyte lineage regardless of Erk expression; 2) Erk-mediated signals may suppress CD2 expression as well as chondrocyte growth.

Conclusions

In this study, we showed that elimination of Erk by CD2-Cre leads to hyperplastic chondrocytes. The scattered CD2 expression in a chondrocyte lineage is naturally occurred in Erk-sufficient condition, leading to the similar frequency and distribution of RFP^+ chondrocyte clusters to those in Erk-deficient mice (Fig. 3E). Thus far, we did not observe apparent morphologic difference between RFP^+ (CD2-expressed) and RFP^- (CD2-non-expressed) chondrocytes. Nevertheless, this suggests that chondrocytes constitute heterogeneous subpopulations that differ in ontogenetic process.

During the preparation of this manuscript, two other groups published related studies. Guittard et al. and Wehenkel et al. reported that CD4-Cre-mediated deletion of Sos1/2 or Erk1/2 both caused similar abnormal chondrocyte hyperplasia (17,18). By using qRT-PCR and fluorescent fate-mapping respectively, they showed the existence of chondrocytes that had CD4 expression, thus proposing that this phenomenon was due to ectopic expression of CD4 in chondrocytes. However, the similar expression pattern of CD2 and chondroma genesis induced by CD2-Cre in our study imply that not only CD4, but also other T cell-related genes may be transiently expressed in some particular cells

during early development of chondrocyte (supplementary Fig. 1). Normally these genes are likely programmed to be extinguished during further chondrocyte maturation, but are sustained in the absence of Ras-Erk pathway (Fig. 3G). Thus, we propose that an unexpected link may exist between T-like cell and chondrocyte lineages during ontogeny. One may argue that the expression of T cell-related genes in chondrocytes is due to physical acquisition of mRNA/protein from neighboring T cells (19), however, it is less likely as chondroma formation occurred in the absence of T cells (Fig. 2D).

In Sos- or Erk-deficient mice created using CD4-Cre, the limb joint nodules were observed mainly at the carpus (17,18). In contrast, our CD2-Cre-driven Erk-deficient mice developed chondromas at the distal and proximal interphalangeal joints (Fig. 1A and 1B). In addition, we did not observe any of the spinal abnormalities seen in CD4-Cre driven Sos- or Erk-deficient mice in our $Erk^{\Delta CD2\text{-}Cre}$ mice (Fig. 1B). Different locations of hyperplastic chondrocytes may be due to the subtly different expression patterns of T cell markers that drive Cre expression in chondrocytes. More detailed studies utilizing precise fate-mapping tracing of chondrocyte lineages in combination with various T cell-related gene-driven multiple deleters, i.e. Cre and Flpe, will further clarify this issue.

It still remains unclear how, when and why T cell markers are expressed in chondrocyte lineage. The physiological consequences of this hypothetic link between T-like cell and chondrocyte lineages are principal issues that require further investigation.

Acknowledgments

We thank T. Yasuda, T. Kurosaki, T. Ishikawa, C. Coban, M. Nagata and Y. Hosono for discussion; M. Kurata, S. Iwai and K. Ichikawa for technical assistance; H. Luche, H-J. Fehling, B. and M. Malissen for providing mice; and M. Tanaka in the Laboratory of Embryonic and Genetic Engineering for animal support. This research was supported by Grant-in-Aid for Scientific Research on Innovative Areas (26110009).

Figure 1. Abnormal cartilage formation in Erk$^{\Delta CD2\text{-}Cre}$ mice.

(A) Images of whole bodies (left), fore feet (upper right), and hind feet (lower right) from WT (67-week-old) and Erk$^{\Delta CD2\text{-}Cre}$ (60-week-old) mice. Arrows indicate nodules.

(B) X-ray images of whole bodies (upper) and hind feet (lower) from WT (41-week-old) and Erk$^{\Delta CD2\text{-}Cre}$ (35-week-old) mice were obtained with an X-ray imaging microscope. The inset images show hind feet in bright-field. White arrows indicate abnormal hard tissues.

(C) Hematoxylin and eosin (HE) staining of forefoot sections from WT and Erk$^{\Delta CD2\text{-}Cre}$ mice. Close up views of boxed areas in the upper panels are shown at the bottom. Scale bars, 1 mm for upper panels; 100 μm for lower panels.

(D) RT-PCR analysis of chondrocyte markers (Sox9, Col2 and Acan) and a hypertrophic chondrocyte marker (Col10) in WT ear auricular cartilage and a finger nodule from Erk$^{\Delta CD2\text{-}Cre}$ mice. GAPDH was used as a control.

Figure 2. T cell-independent chondroma formation in Erk$^{\Delta CD2\text{-}Cre}$ mice.

(A) Mean clinical scores of Erk$^{\Delta CD2\text{-}Cre}$ mice at the ages of 6 to 63 weeks were determined. The detail of the scoring system is described in Methods.

(B) The incidences of chondroma formation in WT (n=8), Erk1$^{-/-}$ (n=5), Erk2$^{\Delta CD2\text{-}Cre}$ (n=27), and Erk1$^{-/-}$Erk2$^{\Delta CD2\text{-}Cre}$ (Erk$^{\Delta CD2\text{-}Cre}$) (n=13) mice older than 20 weeks were presented. The incidence was calculated as described in Methods.

(C) WT mice (n=15) adoptively transferred with Erk$^{\Delta CD2\text{-}Cre}$ BM cells were assessed for chondroma formation at the indicated time points after transfer.

(D) Incidences of chondroma formation in $Erk^{\Delta CD2\text{-}Cre}$ mice and $Erk^{\Delta CD2\text{-}Cre}$ × $CD3\varepsilon^{\Delta 5/\Delta 5}$ mice were determined at the indicated time points.

Figure 3. Evidence for CD2-driven Cre expression in a subpopulation of chondrocytes.

(A) Hind feet of $Erk^{\Delta CD2\text{-}Cre}$ (left) and $Erk^{\Delta CD2\text{-}Cre}$ × ROSA26-STOP-RFP ($Erk^{\Delta CD2\text{-}Cre}$ × R26-RFP) (right) mice were analyzed using bright-field and fluorescence stereomicroscopy.

(B) A nodule on the hind foot of $Erk^{\Delta CD2\text{-}Cre}$ × R26-RFP mice was analyzed after the skin was removed using bright-field and fluorescence stereomicroscopy.

(C) RT-PCR analysis of CD2 mRNA expression in the chondromas from $Erk^{\Delta CD2\text{-}Cre}$ mice and WT splenic T cells. The amplification of CD2 cDNA was performed for 42 cycles (upper panel). GAPDH was analyzed as a control and amplified for 32 cycles (lower panel). Threefold serial dilutions of cDNA were used as templates. W, water.

(D) Genomic PCR for detection of TCRβ rearrangement in the chondromas from $Erk^{\Delta CD2\text{-}Cre}$ mice and WT splenic T cells. The amplification was performed for 30 cycles. Threefold serial dilutions of genomic DNA were used as templates. GL, germline. W, water.

(E) RFP reporter expression in the auricular cartilage from CD2-Cre × R26-RFP (Erk-sufficient) and $Erk^{\Delta CD2\text{-}Cre}$ × R26-RFP (Erk-deficient) mice was observed vertically to the cartilage layer (left panels). Bright-field and merged images are shown in the middle and right panels respectively. Scale bars indicate 100 μm.

(F) RFP reporter expression in cross sections of auricular cartilage from CD2-Cre × R26-RFP (Erk-sufficient) and $Erk^{\Delta CD2\text{-}Cre}$ × R26-RFP (Erk-deficient) mice. Bright-field and merged images are shown in the middle and right panels respectively. Dashed lines indicate chondrocyte layer. Arrows show RFP^{+} chondrocytes. Scale bars indicate 50 μm.

(G) RT-PCR analysis of CD2 mRNA expression in auricular chondrocytes from CD2-Cre × R26-RFP (Erk-sufficient) mice and $Erk^{\Delta CD2\text{-}Cre}$ × R26-RFP (Erk-deficient) mice. Threefold serial dilutions of cDNA were used as templates. GAPDH was analyzed as a control. The amplification was performed for 40 cycles (CD2) and 30 cycles (GAPDH).

Supplementary figure 1. The expression of T cell markers in chondroma.

RT-PCR analysis of T cell markers in chondromas from $Erk^{\Delta CD2\text{-}Cre}$ mice and WT splenic T cells. Threefold serial dilutions of cDNA were used as templates. GAPDH was analyzed as a control. The amplification was performed for 40 cycles (CD4, CD3, CD8 and Lck) and 30 cycles (GAPDH).

References

1 de Boer, J., Williams, A., Skavdis, G., Harker, N., Coles, M., Tolaini, M., Norton, T., Williams, K., Roderick, K., Potocnik, A. J., and Kioussis, D. 2003. Transgenic mice with hematopoietic and lymphoid specific expression of Cre. *Eur. J. Immunol.* 33:314.

2 Sawada, S., Scarborough, J. D., Killeen, N., and Littman, D. R. 1994. A lineage-specific transcriptional silencer regulates CD4 gene expression during T lymphocyte development. *Cell* 77:917.

3 Garvin, A. M., Abraham, K. M., Forbush, K. A., Farr, A. G., Davison, B. L., and Perlmutter, R. M. 1990. Disruption of thymocyte development and lymphomagenesis induced by SV40 T-antigen. *Int. Immunol.* 2:173.

4 Roncagalli, R., Hauri, S., Fiore, F., Liang, Y., Chen, Z., Sansoni, A., Kanduri, K., Joly, R., Malzac, A., Lahdesmaki, H., Lahesmaa, R., Yamasaki, S., Saito, T., Malissen, M., Aebersold, R., Gstaiger, M., and Malissen, B. 2014. Quantitative proteomics analysis of signalosome dynamics in primary T cells identifies the surface receptor CD6 as a Lat adaptor-independent TCR signaling hub. *Nat. Immunol.* 15:384.

5 Giordano, M., Roncagalli, R., Bourdely, P., Chasson, L., Buferne, M., Yamasaki, S., Beyaert, R., van Loo, G., Auphan-Anezin, N., Schmitt-Verhulst, A. M., and Verdeil, G. 2014. The tumor necrosis factor alpha-induced protein 3 (TNFAIP3, A20) imposes a brake on antitumor activity of CD8 T cells. *Proc. Natl Acad. Sci. USA* 111:11115.

6 Pages, G., Lenormand, P., L'Allemain, G., Chambard, J. C., Meloche, S., and Pouysségur, J. 1993. Mitogen-activated protein kinases p42mapk and p44mapk are required for fibroblast proliferation. *Proc. Natl Acad. Sci. USA* 90:8319.

7 Yoon, S. and Seger, R. 2006. The extracellular signal-regulated kinase: multiple substrates regulate diverse cellular functions. *Growth Factors* 24:21.

8 Oh, C. D., Chang, S. H., Yoon, Y. M., Lee, S. J., Lee, Y. S., Kang, S. S., and Chun, J. S. 2000. Opposing role of mitogen-activated protein kinase subtypes, erk-1/2 and p38, in the regulation of chondrogenesis of mesenchymes. *J. Biol. Chem.* 275:5613.

9 Bobick, B. E. and Kulyk, W. M. 2004. The MEK-ERK signaling pathway is a negative regulator of cartilage-specific gene expression in embryonic limb

mesenchyme. *J. Biol. Chem.* 279:4588.

10 Matsushita, T., Chan, Y. Y., Kawanami, A., Balmes, G., Landreth, G. E., and Murakami, S. 2009. Extracellular signal-regulated kinase 1 (ERK1) and ERK2 play essential roles in osteoblast differentiation and in supporting osteoclastogenesis. *Mol. Cell. Biol.* 29:5843.

11 Murakami, S., Balmes, G., McKinney, S., Zhang, Z., Givol, D., and de Crombrugghe, B. 2004. Constitutive activation of MEK1 in chondrocytes causes Stat1-independent achondroplasia-like dwarfism and rescues the Fgfr3-deficient mouse phenotype. *Genes. Dev.* 18:290.

12 Pages, G., Guerin, S., Grall, D., Bonino, F., Smith, A., Anjuere, F., Auberger, P., and Pouyssegur, J. 1999. Defective thymocyte maturation in p44 MAP kinase (Erk 1) knockout mice. *Science* 286:1374.

13 Hatano, N., Mori, Y., Oh-hora, M., Kosugi, A., Fujikawa, T., Nakai, N., Niwa, H., Miyazaki, J., Hamaoka, T., and Ogata, M. 2003. Essential role for ERK2 mitogen-activated protein kinase in placental development. *Genes Cells.* 8:847.

14 Luche, H., Weber, O., Nageswara Rao, T., Blum, C., and Fehling, H. J. 2007. Faithful activation of an extra-bright red fluorescent protein in "knock-in" Cre-reporter mice ideally suited for lineage tracing studies. *Eur. J. Immunol.* 37:43.

15 Malissen, M., Gillet, A., Ardouin, L., Bouvier, G., Trucy, J., Ferrier, P., Vivier, E., and Malissen, B. 1995. Altered T cell development in mice with a targeted mutation of the CD3-epsilon gene. *EMBO J.* 14:4641.

16 Sebastian, A., Matsushita, T., Kawanami, A., Mackem, S., Landreth, G. E., and Murakami, S. 2011. Genetic inactivation of ERK1 and ERK2 in chondrocytes promotes bone growth and enlarges the spinal canal. *J. Orthop. Res.* 29:375.

17 Guittard, G., Gallardo, D. L., Li, W., Melis, N., Lui, J. C., Kortum, R. L., Shakarishvili, N. G., Huh, S., Baron, J., Weigert, R., Kramer, J. A., Samelson, L. E., and Sommers, C. L. 2017. Unexpected Cartilage Phenotype in CD4-CRE-Conditional SOS-Deficient Mice. *Front. Immunol.* 8:343.

18 Wehenkel, M., Corr, M., Guy, C. S., Edwards, B. A., Castellaw, A. H., Calabrese, C., Pages, G., Pouyssegur, J., Vogel, P., and McGargill, M. A. 2017. Extracellular Signal-Regulated Kinase Signaling in CD4-Expressing Cells Inhibits Osteochondromas. *Front. Immunol.* 8:482.

19 Miyake, K., Shiozawa, N., Nagao, T., Yoshikawa, S., Yamanishi, Y., and Karasuyama, H. 2017. Trogocytosis of peptide-MHC class II complexes from dendritic cells confers antigen-presenting ability on basophils. *Proc. Natl Acad. Sci. USA* 114:1111.

Figure 1

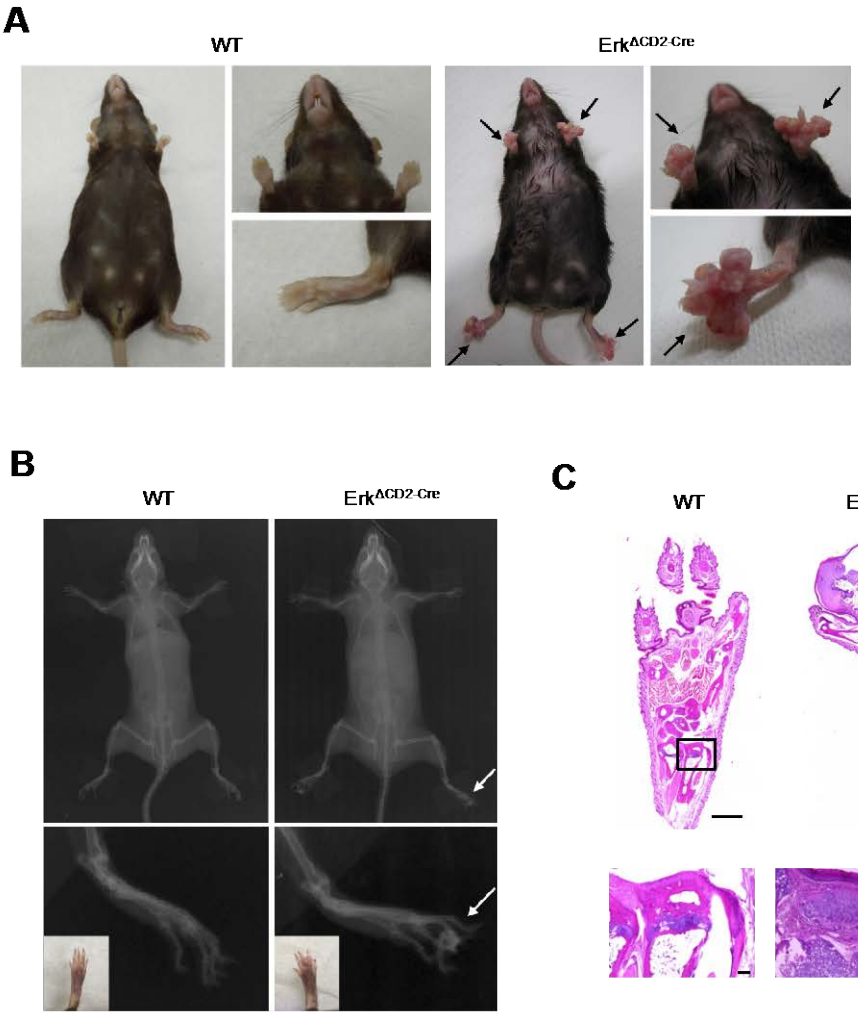
A
WT
Erk^ΔCD2-Cre
B
WT
Erk^ΔCD2-Cre
C
WT
Erk^ΔCD2-Cre
D
Water
Ear auricular chondrocytes
Finger chondroma
Sox9
Col2
Acan
Col10
Gapdh

Figure 2

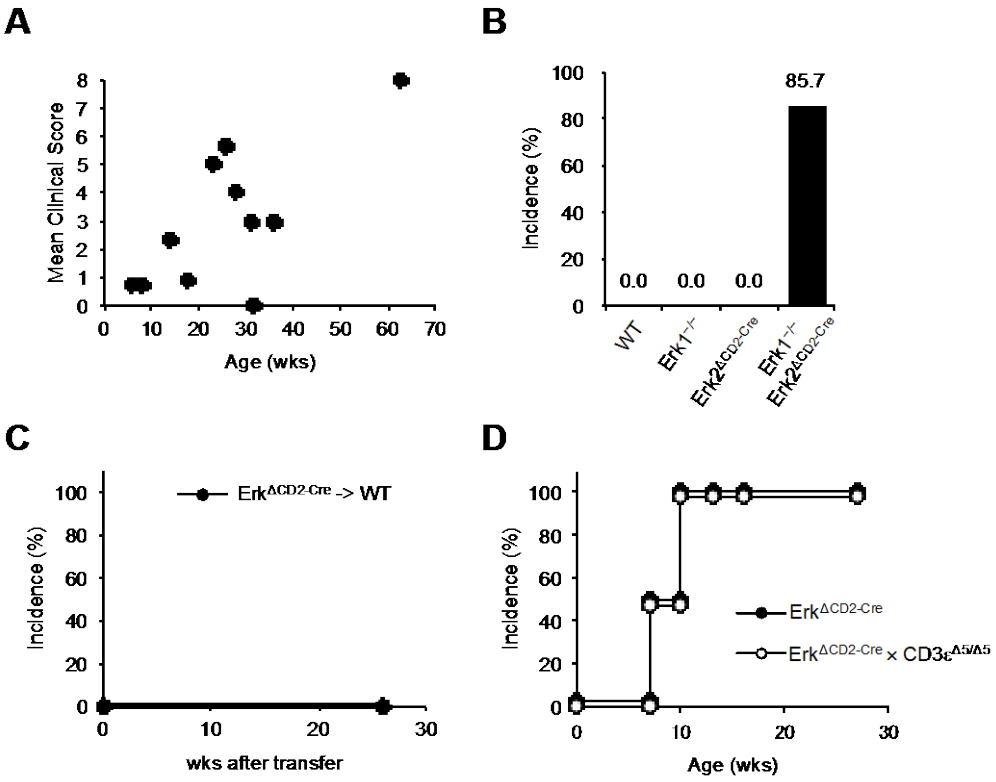
A
Mean Clinical Score
Age (wks)
B
Incidence (%)
85.7
0.0
0.0
0.0
WT
Erk1−/−
Erk2ΔCD2-Cre
Erk1−/− Erk2ΔCD2-Cre
C
Incidence (%)
ErkΔCD2-Cre -> WT
wks after transfer
D
Incidence (%)
ErkΔCD2-Cre
ErkΔCD2-Cre × CD3εΔ5/Δ5
Age (wks)

Figure 3

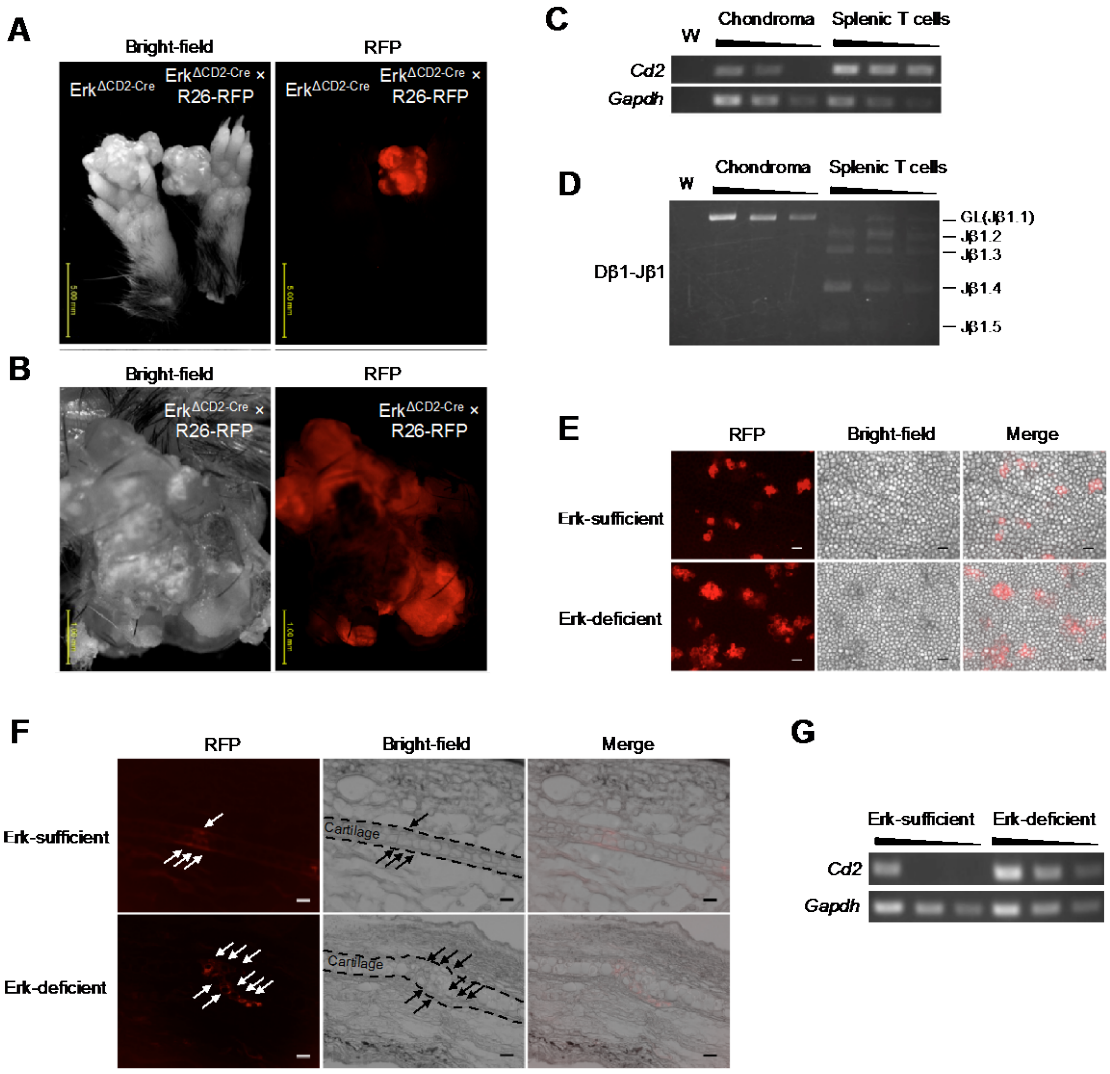
A
Bright-field
RFP
Erk^ΔCD2-Cre
Erk^ΔCD2-Cre × R26-RFP
B
C
W
Chondroma
Splenic T cells
Cd2
Gapdh
D
Dβ1-Jβ1
GL(Jβ1.1)
Jβ1.2
Jβ1.3
Jβ1.4
Jβ1.5
E
RFP
Bright-field
Merge
Erk-sufficient
Erk-deficient
F
Cartilage
G

Supplementary Figure 1